OncoTargets and Therapy

Dovepress
open access to scientific and medical research

Open Access Full Text Article

ORIGINAL RESEARCH

RETRACTED ARTICLE: LncRNA EWSAT1 Promotes Colorectal Cancer Progression Through Sponging miR-326 to Modulate FBXL20 Expression

This article was published in the following Dove Press journal:
OncoTargets and Therapy

Jing Liu[1,*]
Shimei Huang[2,*]
Xin Liao[1]
Zhongsheng Chen[3]
Lianghe Li[3]
Lei Yu[4]
Wei Zhan[5]
Rui Li[6]

[1]Imaging Department, Affiliated Hospital of Guizhou Medical University, Guiyang, People's Republic of China; [2]Forensic Clinical Teaching and Research Office, Guizhou Medical University, Guiyang, People's Republic of China; [3]Surgery, Guizhou Medical University, Guiyang, People's Republic of China; [4]Department of Pathology, Guiyang Maternal and Child Health Hospital, Guiyang, People's Republic of China; [5]General Surgery, Affiliated Hospital of Guizhou Medical University, Guiyang, People's Republic of China; [6]Department of Traditional Chinese Medicine, Guizhou Provincial People's Hospital, Guiyang, People's Republic of China

*These authors contributed equally to this work

Background: Ewing sarcoma-associated transcript 1 (*EWSAT1*) has been reported to be a pivotal modulator in a series of cancers. However, the function of *EWSAT1* in colorectal cancer (CRC) has not been elaborated. This study aimed to explore the role of *EWSAT1* in CRC progression and the underlying mechanisms.

Methods: The expression patterns of *EWSAT1*, *miR-326* and *FBXL20* were examined by qCRCR. Si-EWSAT1 was transfected to study the effects of *EWSAT1* on cell proliferation and metastasis. Rescue experiments were performed to investigate the underlying mechanisms in vitro. Xenograft models were used to evaluate the role of *EWSAT1* in vivo.

Results: We found that *EWSAT1* was highly expressed in CRC tissues and cell lines and associated with poor overall survival. In vitro, knockdown of *EWSAT1* suppressed the cell proliferation, migration and invasion. Moreover, miR-326 was found to be a target of *EWSAT1*, and *miR-326* inhibitor could partially reverse the effects on CRC cell progression induced by si-EWSAT1. Subsequently, we validated *FBXL20* as a vital downstream target for *miR-326*, and *EWSAT1* positively regulated *FBXL20* via *miR-326* in vitro. In addition, these findings were confirmed by in vivo experiments.

Conclusion: Taken together, the data showed that *EWSAT1* promoted CRC progression via targeting *miR-326/FBXL20* pathway, which might provide a novel therapeutic target for CRC treatment.

Keywords: *lncRNA EWSAT1*, colorectal cancer, CRC, *miR-326*, *FBXL20*

Introduction

Colorectal cancer (CRC) is a common malignancy and causes about one million deaths every year.[1] In China, the incidence rate of colorectal cancer increases, and an upward trend of mortality rate is also observed.[2] In spite of efforts made in CRC treatment, the overall 5-year survival remains less than 30%.[3] The poor 5-year survival rate is largely due to the fact that we cannot diagnose CRC before it enters advanced stage. Thus, there is an urgent need to know the pathogenesis of CRC and find out the biomarker involved in this disease.

Long non-coding RNAs (lncRNAs) are a group of non-coding RNAs with a length longer than 200 nt.[4] Increasing evidence revealed that dysregulated lncRNAs in multiple types of cancers are responsible for cell proliferation and metastasis.[5] LncRNA Ewing sarcoma-associated transcript 1 (*EWSAT1*) was located on chromosome 15 between two protein-coding genes. *EWSAT1* was first discovered to play roles in Ewing sarcoma development.[6] Thereafter, emerging evidence revealed

Correspondence: Rui Li
Department of Traditional Chinese Medicine, Guizhou Provincial People's Hospital, Zhongshan East Road 83, Guiyang 550002, People's Republic of China
Email ruilidoctor@126.com

submit your manuscript | www.dovepress.com
DovePress
http://doi.org/10.2147/OTT.S272895

that *EWSAT1* was highly expressed and exerted oncogenic roles in a series of cancer types, such as nasopharyngeal carcinoma,[7] cervical cancer,[8] osteosarcoma,[9] and ovarian cancer.[10] However, the role of *EWSAT1* in colorectal cancer was not elaborated. Thus, we speculated that *EWSAT1* might also paly roles in colorectal cancer. We detected the expression levels of *EWSAT1* in tumor tissues from colorectal cancer patients, and observed the overexpression of *EWSAT1*, compared to the adjacent normal tissues. The above findings made us to investigate the role of EWSAT1 in colorectal cancer progression.

LncRNAs usually function by acting as competing endogenous RNAs (ceRNAs) for microRNAs, thus regulating the downstream target genes at post-transcriptional level.[11] LncRNAs exhibit tumor-suppressive or oncogenic functions in multiple cancer types, including colorectal cancer.[12–14] Moreover, a series of lncRNAs are reported to regulate colorectal cancer development via sponging miRNAs. For example, lncRNA PART1 inhibited miR-150-5p thereby upregulating LRG1 to promote colorectal cancer development.[8] *SBF2-AS1* driven colorectal cancer via regulating miR-619-5p/HDAC3 axis.[15] Depletion of SNHG14 inhibited CRC cell proliferation in vitro by modulating miR-32-5p/SKIL axis.[16] However, the relationship between EWSAT1 and miRNAs in CRC was unknown.

In this work, we demonstrated that *EWSAT1* was highly expressed in CRC tissues and cell lines, and contributed to the poor characteristics of CRC patients. EWSAT1 knockdown suppressed cell proliferation, migration and invasion in vitro, and suppressed tumorigenesis in vivo. Additionally, we found that the oncogenic effects of EWSAT1 on CRC were through regulating the miR-326/FBXL20 axis.

Methods

Patients and Tissue Samples

A total of 45-paired CRC tissues and adjacent normal tissues were collected from patients who underwent surgical resection at the First Affiliated Hospital of Zhengzhou University. The samples were immediately frozen in liquid nitrogen and stored at −80 °C for the following experiments. Clinicopathological characteristics are presented in Table 1. None of the patients had received local or systemic treatment. Informed written consents were collected from every patient included in this study. The protocol of

Table 1 Association Between EWSAT1 Expression and Clinicopathological Characteristics of Colorectal Cancer Patients

Characteristics Total	N=45	EWSAT1 Expression		P value
		High (n=30)	Low (n=15)	
Age (years)				
≥65	34	26	8	0.589
<65	11	4	7	
Gleason score				
≥7	26	18	8	0.016*
<7	19	13	6	
Tumor stage				
T2	18	10	8	0.029*
T3-T4	27	20	7	
Lymph-node metastasis				
Yes	21	17	4	0.092
No	24	16	8	
Tumor size (cm)				
>2.5	24	18	6	0.165
≤2.5	21	12	7	
Multiple lesions				
Positive	25	16	9	0.718
Negative	20	15	5	

Note: *P < 0.05 represents statistical differences.

Table 2 Primers of qRT-PCR

Gene	Primers	
EWSAT1	Forward Reverse	5-GTGTCTGGCAAGGAACACTA-3' 5'-GGTGGAGAAGAGGGACAATAAG-3'
miR-326	Stem-loop RT primer Forward Reverse	5'-GTCGTATCCAGTGCAGGGTCCGAGGTATTCGCACTGGTACGACCUGGAG -3' 5'-CCUCUGGGCCCUUC-3' 5'-GTGCAGGGTCCGAGGT-3'
FBXL20	Forward Reverse	5'-ATGGCCTTAGCTTAGGCT-3' 5'-TTGGCAATGCCGTATTAGC-3'
GAPDH	Forward Reverse	5'-AGCCACATCGCTCAGACAC-3' 5'-GCCCAATACGACCAAATCC-3'
U6	Forward Reverse	5'-GCTTCGGCAGCACATATACTAAAAT-3' 5'-CGCTTCACGAATTTGCGTGTCAT-3'

this study was approved by the Ethics Committee of Guizhou Medical University.

Cell Culture

Human colorectal cancer cell lines (HT-29, SW620, Lovo and SW480), normal colorectal epithelial cell line (NCM460) and HEK-293T cell line were all purchased from ATCC (USA). Cells were incubated in DMEM (Hyclone, USA) medium supplemented with 10% FBS at 37 °C with 5% CO_2.

RNA Extraction and Quantitative Real-Time CRCR (qRT-CRCR)

Total RNA was extracted using Trizol (Invitrogen, USA), according to the manufacturer's protocol. Reverse Transcription Kit (Takara, Dalian, China) was used to transcribe RNA into cDNA reversely. qCRCR was carried out via SYBR Green One-Step RT-qCRCR Kit (Solarbio, Shanghai, China). GAPDH and U6 were chosen to be internal controls for mRNA and miRNAs, respectively. Data were analyzed by the $2^{-\Delta\Delta Ct}$ method and each sample was repeated three times. Table 2 presents the sequences of primers.

Cell Transfection

Si-EWSAT1, miR-326 inhibitor, miR-326 mimics and their negative controls were provided by Promega (Nanjing, China), and were transfected into cells with Lipo2000 (Invitrogen, Jinan, China) in accordance with the protocol.

CCK-8 Assay

Cells were plated in 96-well plates (1×10^3 cells/well), and incubated with complete medium. After every 24 h, CCK-8 solution was added into each well and a microplate reader was taken to analyze the absorbance at 450 nm.

Cell Colony Assay

Cells were plated in 6-well plate and incubated in complete medium for 2 weeks. Medium was replaced every 3 days. After then, cells were stained by crystal violet (Promega, Wuhan), photographed and counted.

Wound Healing Assay

Cell migration rate was analyzed by wound healing assay. In brief, a scratch was made across the surface of cells by a new micropipette tip. Twenty-four hours later, the state of the wounds was observed by an inverted microscope (Olympus, Japan).

Transwell Assay

A 24-well insert transwell chamber (BD Biosciences, USA) was taken to detect the cell invasion. Transfected cells were plated onto the upper chamber coated with Matrigel. Complete medium containing 10% FBS (Gibico, USA) was added into the bottom chamber. The cells were incubated for 24 h, and 20% methanol and 0.1% crystal violet were added to the lower chamber. The invaded cells were stained by crystal violet and counted from six randomly visual fields.

RNA Immunoprecipitation (RIP)

The RIP assay was carried out using the Imprint RNA Immunoprecipitation Kit (Sigma, USA), according to the manufacturer's protocol. Antibodies are as follows: anti-Ago2

(CST, Shanghai, China) and anti-IgG (CST, Shanghai, China). Purified RNA was isolated for qRT-CRCR experiments.

Western Blot

Total protein was isolated from cells or tissues by RIPA buffer (Sigma, USA) in accordance with the protocol. Equal amounts were loaded and separated by 10% SDS-PAGE. Proteins were transferred from gel to PVDF membrane (Millipore, USA) and blocked with 5% silk milk for 2h at room temperature. Thereafter, membranes were incubated in primary antibodies: anti-FBLX20 antibody (Abcam, 1:500), anti-GAPDH antibody (CST, 1:2000).

Immunohistochemistry Assay (IHC)

Xenograft tumor tissues were fixed with 10% formaldehyde and sectioned into 4-μm thick. Samples were incubated with the primary anti-Ki-67 antibody (CST, 1:800) at 4 °C overnight. Secondary HRP-conjugated anti-Rabbit antibody was added the next day and the signals were developed using DAB plus kit.

Animal Models

Xenograft models were established by injecting SW480 cells expressing sh-EWSAT1 or sh-NC stably into nude mice. Tumor size was estimated every week, and 5 weeks later, mice were sacrificed for tumor weight detection and downstream experiments. The studies were approved by the Ethics Committee of Guizhou Medical University and carried out in accordance with the Guidelines for Animal Use in the National Institutes of Health.

Statistical Analysis

Data were presented as mean ±SD from at least three repeated experiments. Statistical analysis was performed by SPSS 17.0, together with generating the graphs using GraphPad Prism 5.0. The difference between the two groups was analyzed via the Student's *t* test. Differences among multiple groups were analyzed via one-way ANOVA. Overall survival curve was determined by Kaplan-Meier survival analysis. Correlation analysis was analyzed via Pearson's correlation analysis. $P < 0.05$ was considered to be statistically significant.

Result

Upregulation of EWSAT1 in CRC Tissues and Cell Lines

To explore the role of *EWSAT1* in CRC, we first detected the expression of *EWSAT1* in CRC tissues and cell lines. As shown in Figure 1A, *EWSAT1* was upregulated in CRC cancer tissues, whereas downregulated in adjacent normal tissues. We also evaluated *EWSAT1* expression levels in CRC tumor tissues (n = 279) and normal colorectal tissues (n = 41) from TCGA databases and found that *EWSAT1* was highly expressed in CRC tumor samples (Figure S1). Figure 1B shows that *EWSAT1* was also upregulated in CRC cell lines (HT-29, SW620, Lovo and SW480), whereas downregulated in normal osteoblasts (RWPE cells). Additionally, patients with higher *EWSAT1* overexpression associated with poorer overall survival (Figure 1C). These results led us to propose that *EWSAT1* might play roles in CRC progression.

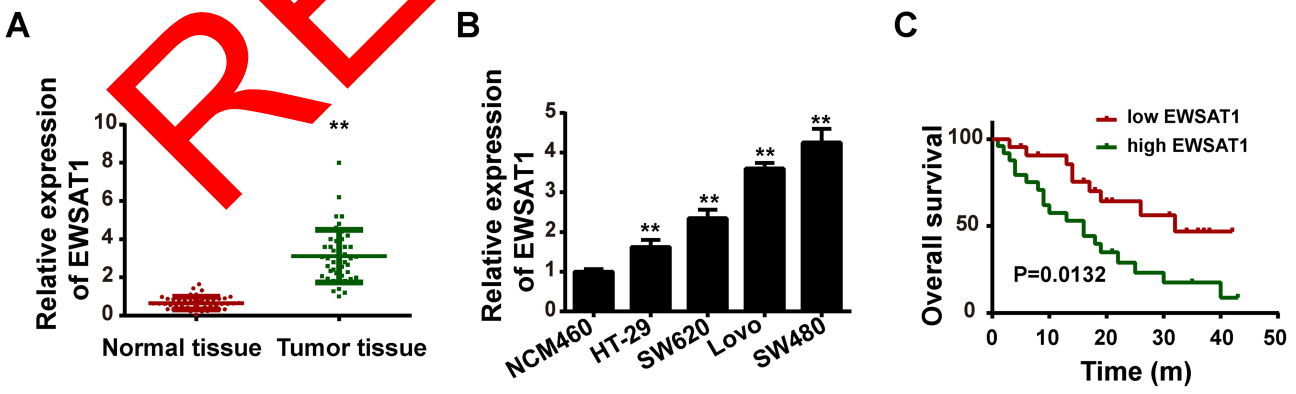

Figure 1 EWSAT1 was overexpressed in CRC tissue samples and cell lines. (**A**) Relative expressions of EWSAT1 in CRC tissues and paired normal ones were analyzed by RT-qCRCR. (**B**) Relative expressions of EWSAT1 in four CRC cell lines (LNCap, C4-2, CRC-3 and Du-145) and a normal cell line (RWPE) were analyzed by RT-qCRCR. (**C**) Association between high EWSAT1 expression and unfavorable prognosis in CRC patients was analyzed by Kaplan–Meier survival analysis. **P < 0.01 vs normal tissue or RWPE cells.

EWSAT1 Knockdown Restricted CRC Cell Proliferation, Migration and Invasion in vitro

To evaluate the effects of *EWSAT1* on CRC progression, we conducted loss-of-function experiments. We first checked the knockdown efficiency of si-EWSAT1 by transfecting two siRNAs (si-EWSAT1#1 and s-EWSAT1#2) targeting *EWSAT1* into CRC cell lines. The results showed that both the two si-EWSAT1s exerted significant knockdown efficiency (Figure 2A), and we chose EWSAT1#2 for the following experiments. The CCK-8 and colony assays proved that CRC cells transfected with si-EWSAT1 exhibited decreased

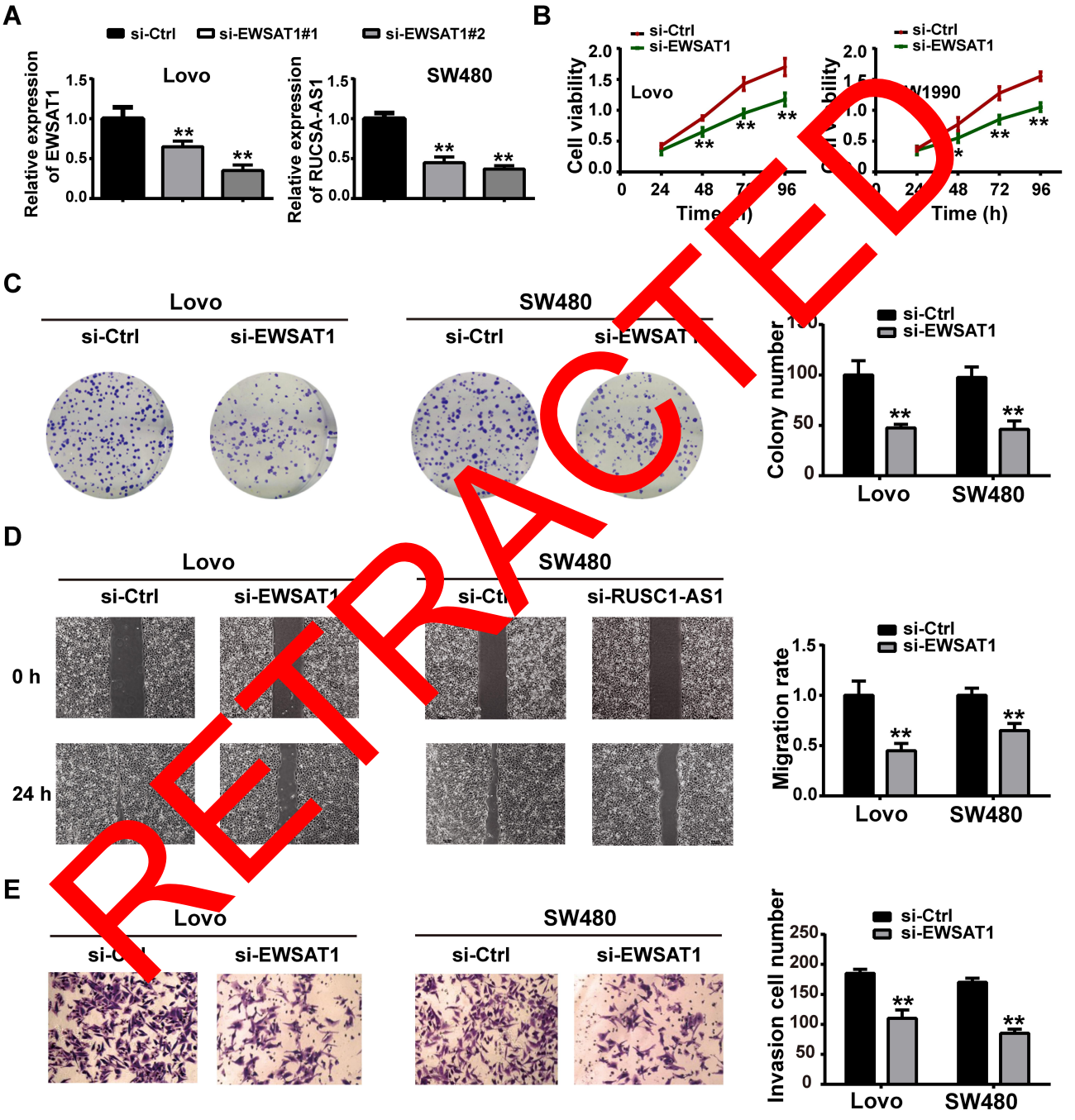

Figure 2 Knockdown of *EWSAT1* inhibited the proliferation, migration and invasion of CRC-3 and Du-145 cells. (**A**) *EWSAT1* expression was estimated by qCRCR after transfection with two si-RNAs targeting *EWSAT1* (si-EWSAT1#1 and si-EWSAT1#2), showing the significant knockdown efficiency. (**B**) Grown curves were performed via CCK-8 assay, after transfection with si-EWSAT1 for 24h, 48h, 72h and 96h. (**C**) Colony assay was carried out to determine the effect of *EWSAT1* knockdown on cell proliferation. (**D**) Wound healing assay was performed to estimate the effect of *EWSAT1* knockdown on cell migration. (**E**) Transwell assay was performed to analyzed the effect of *EWSAT1* knockdown on cell invasion. *P<0.05, vs si-Ctrl; **P < 0.01 vs si-Ctrl.

proliferation (Figure 2B–C). Moreover, we performed wound healing assay and transwell assay to determine the effects of si-EWSAT1 on CRC cell metastasis. As shown in Figure 2D–E, the migrating rate and invasion number of CRC cells were both downregulated by si-EWSAT1 transfection.

EWSAT1 Directly Interacted with miR-326

As lncRNAs often acted as ceRNAs for corresponding miRNAs, we took Starbase v2.0 to predict miR-326 as the candidate miRNA which might be inactivated by *EWSAT1*. Figure 3A presents the predicted binding sites, which was validated by the following luciferase reporter assay (Figure 3B). Moreover, miR-326 was upregulated upon si-EWSAT1 transfection (Figure 3C), and *EWSAT1* was also downregulated with miR-326 overexpression (Figure 3D). RIP assay with antibody targeting *Ago2* was further performed to demonstrate the direct interaction between *EWSAT1* and *miR-326*. *EWSAT1* and *miR-326*

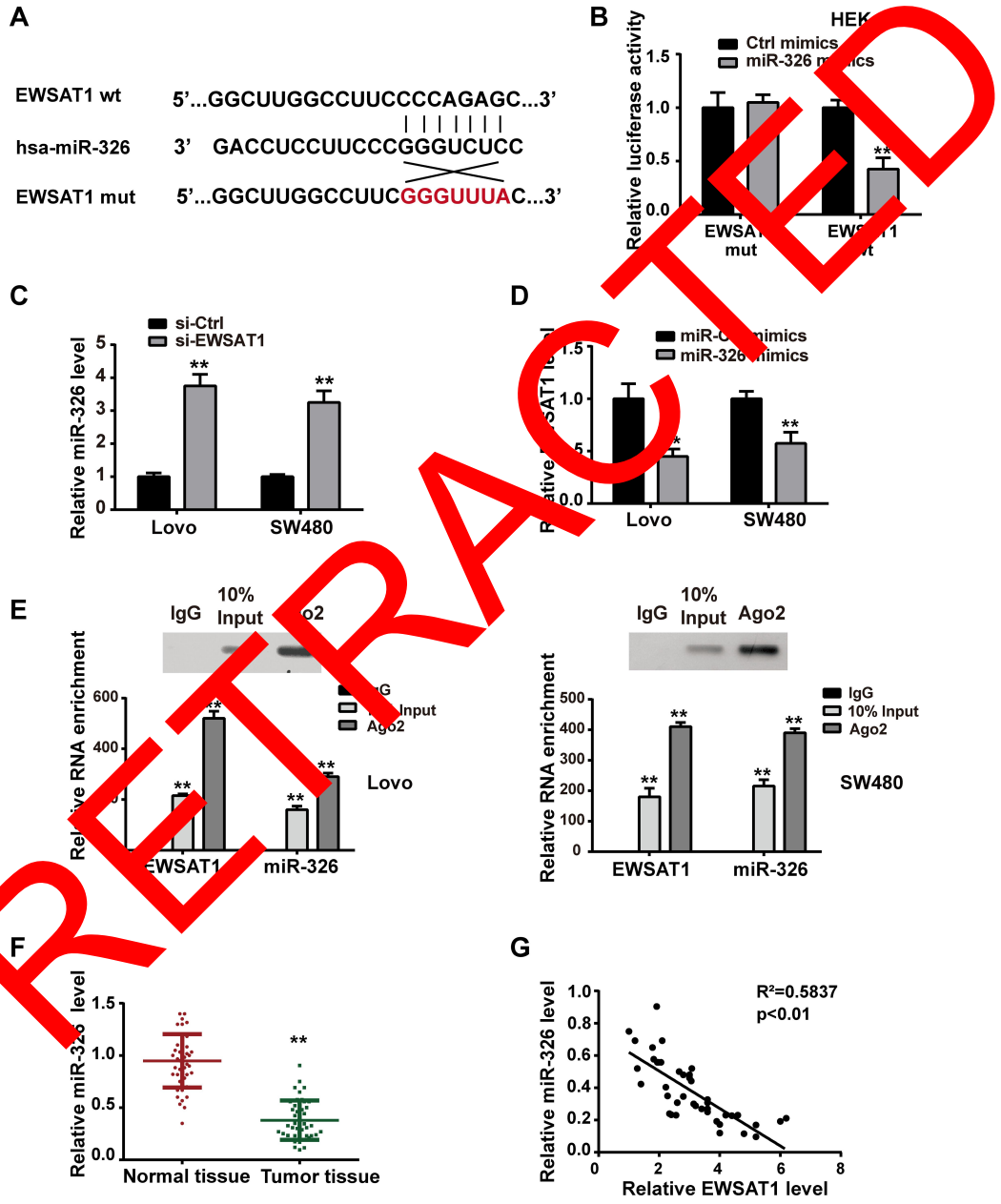

Figure 3 *EWSAT1* inversely interacted with *miR-362*. (**A**) Targeting sites between *EWSAT1* and *miR-326* predicted by Starbase v2.0 were shown. (**B**) Luciferase report assay was performed in HEK-293T cells to verify the predicted binding sites. (**C**) *miR-326* expression was analyzed by qCRCR with si-*EWSAT1* transfection. (**D**) *EWSAT1* expression was measured by qCRCR with *miR-326* mimics transfection. (**E**) Anti-Ago2 RIP assay was performed in CRC-3 and Du-145 cells to determine the direct interaction between *EWSAT1* and *miR-326* in the *Ago2* complex. (**F**) Relative expression of *miR-326* in CRC tissues and paired normal ones were detected by qCRCR. (**G**) Negative correlation between *EWSAT1* and *miR-326* in CRC tissues was analyzed by Pearson analysis. **P < 0.01 vs miR-Ctrl mimics, si-Ctrl, IgG or normal tissue.

were found enriched in *Ago2* complex (Figure 3E). Additionally, we analyzed the *miR-326* level in tissues and found that *miR-326* was lowly expressed in CRC tissues in comparison with that in normal tissues (Figure 3F). Pearson analysis suggested that *miR-326* was negatively correlated with *EWSAT1* in OS tissues (Figure 3G).

EWSAT1 Regulated CRC Cell Proliferation, Migration and Invasion by Sponging miR-326

To further investigate whether the oncogenic effects of *EWSAT1* were mediated by *miR-326*, we performed the rescue experiments. After confirming the knockdown efficiency of *miR-326* inhibitor (Figure 4A), si-EWSAT1 was co-transfected into CRC cells with either Ctrl-inhibitor or miR-326 inhibitor. The following CCK-8 and colony assays demonstrated that the cell viability and proliferation were reduced by si-EWSAT1 and reversed partially by *miR-326* inhibitor (Figure 4B–C). Consistently, the wound healing and transwell assays showed that si-EWSAT1 downregulated the cell migration and invasion; however, *miR-326* inhibitor mitigated the alterations (Figure 4D–E). Figure 4F shows the quantitative results.

miR-326 Directly Targeted FBXL20

By means of target prediction software, we focused on *FBXL20*, which is the potential candidate target of *miR-326*. The predicted binding sites between them are shown in Figure 5A. Luciferase reporter assay was performed in HEK-293T and verified that *FBXL20* was the target of *miR-326* (Figure 5B). Thereafter, we examined the expression level of *FBXL20* with *miR-326* mimics transfection. Q-CRCR and Western blot assays showed that both mRNA and protein expression levels of *FBXL20* were decreased upon *miR-326* overexpression (Figure 5C–D). Furtherly, we analyzed the expression profile of *FBXL20* in patient tissues. We found that *FBXL20* was highly expressed in CRC tissues, whereas lowly expressed in adjacent normal tissues (Figure 5E). The upregulation of *FBXL20* mRNA was negatively correlated with *miR-326* in CRC tumor samples (Figure 5F).

EWSAT1 Positively Regulated FBXL20 Through Modulating miR-326

As we found that *EWSAT1* sponged *miR-326*, and *miR-326* targeted *FBXL20* previously, herein we wanted to explore whether *EWSAT1* could regulate *FBXL20* via *miR-326*. We co-transfected si-EWSAT1 with either miR-Ctrl inhibitor or *miR-326* inhibitor, and the results showed that si-*EWSAT1* reduced mRNA and protein levels of *FBXL20*, while *miR-326* inhibitor reversed the reductions (Figure 6A–C). Notably, the Pearson's correlation analysis revealed that there was a positive correlation between *EWSAT1* and *FBXL20* expressions in CRC tissues (Figure 6D).

Depletion of EWSAT1 Suppressed CRC Tumorigenesis by Upregulating miR-326 and Reducing FBXL20 Expression in vivo

Xenograft models were established to assess the oncogenic effects of *EWSAT1* in vivo. SW480 cells stably transfected with sh-EWSAT1 or sh-Ctrl were injected into the flank of nude mice. We measured the tumor size weekly and found that the growth rate in sh-EWSAT1 was markedly slower than that in the sh-Ctrl group (Figure 7A). After 5 weeks, we analyzed the tumor weight. Consistent with the size, the tumor of sh-EWSAT1 was lighter than that in the sh-Ctrl group (Figure 7B). Moreover, compared to the sh-Ctrl group, the q-CRCR assay demonstrated that miR-326 was upregulated in sh-EWSAT1 mice (Figure 7C), and *FBXL20* protein expression was downregulated in sh-EWSAT1 mice (Figure 7D). Additionally, the expression of *Ki67* detected by ICH was upregulated in sh-EWSAT1 mice, compared with the sh-Ctrl group (Figure 7E). Collectively, these results indicated that *EWSAT1* regulated tumorigenesis via *miR-326* and *FBXL20* in vivo.

Discussion

Increasing studies have revealed the pivotal roles of lncRNAs in multiple physiological and pathological processes, especially in cancers.[17–19] *EWSAT1* has been revealed as an oncogenic gene in a series of cancers. For example, Marques et al first found abnormal expression pattern of *EWAS1* in Ewing sarcoma tissues, and revealed its effects on Ewing sarcoma progression.[6] Subsequently, *EWSAT1* was found to facilitate nasopharyngeal cancer cell proliferation in vitro via sponging *miR-330-5p*.[7] Fu et al revealed that *EWSAT1* was overexpressed in ovarian cancer tissues and promoted cell proliferation via targeting *miR-330-5p*.[10] Zhang et al demonstrated that *EWSAT1* acted as a novel prognostic biomarker in osteosarcoma.[20]

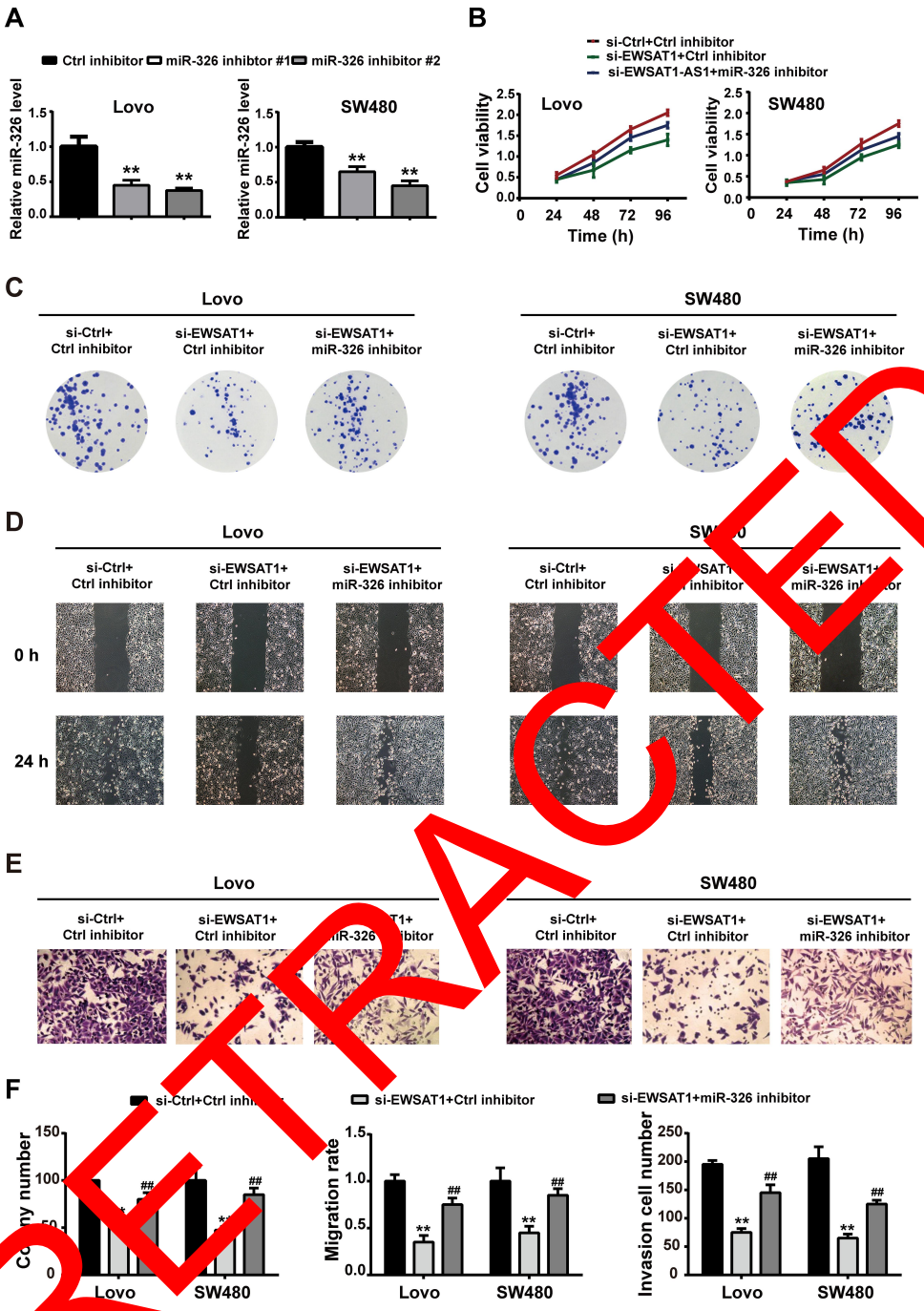

Figure 4 *EWSAT1* [illegible]ulated cell proliferation, migration and invasion via sponging *miR-326*. (**A**) *miR-326* expression was measured with two *miR-326* inhibitors transfection. si-EWSAT[illegible]s transfected with/without the presence of *miR-326*, then (**B**) grown curves were performed by CCK-8 assay; (**C**) colony assay was carried out to determine the effec[illegible] cell proliferation; (**D**) wound healing assay was performed to estimate the effect on cell migration; (**E**) Transwell assay was performed to analyzed the effect on cell invasion. (**F**) Quantitative analysis of colony assay, wound healing assay and transwell assay were presented. **P < 0.01 vs Ctrl inhibitor or si-Ctrl +Ctrl inhibitor; ##P < 0.01 vs si-EWSAT1+Ctrl inhibitor.

In this study, we revealed that *EWSAT1* was upregulated in CRC tissues and cell lines. Knockdown of *EWSAT1* suppressed CRC cell proliferation, migration and invasion in vitro. We overexpressed *EWSAT1*, and detected the effects on CRC cell proliferation, migration and invasion in vitro. However, no evident changes were observed after overexpression of *EWSAT1*. We suspected that the reason is that the expression level of *EWSAT1* was very high already; thus, there was no significant effect after we further upregulated *EWSAT1* expression. These findings suggested the oncogenic role of EWSA1 in CRC development.

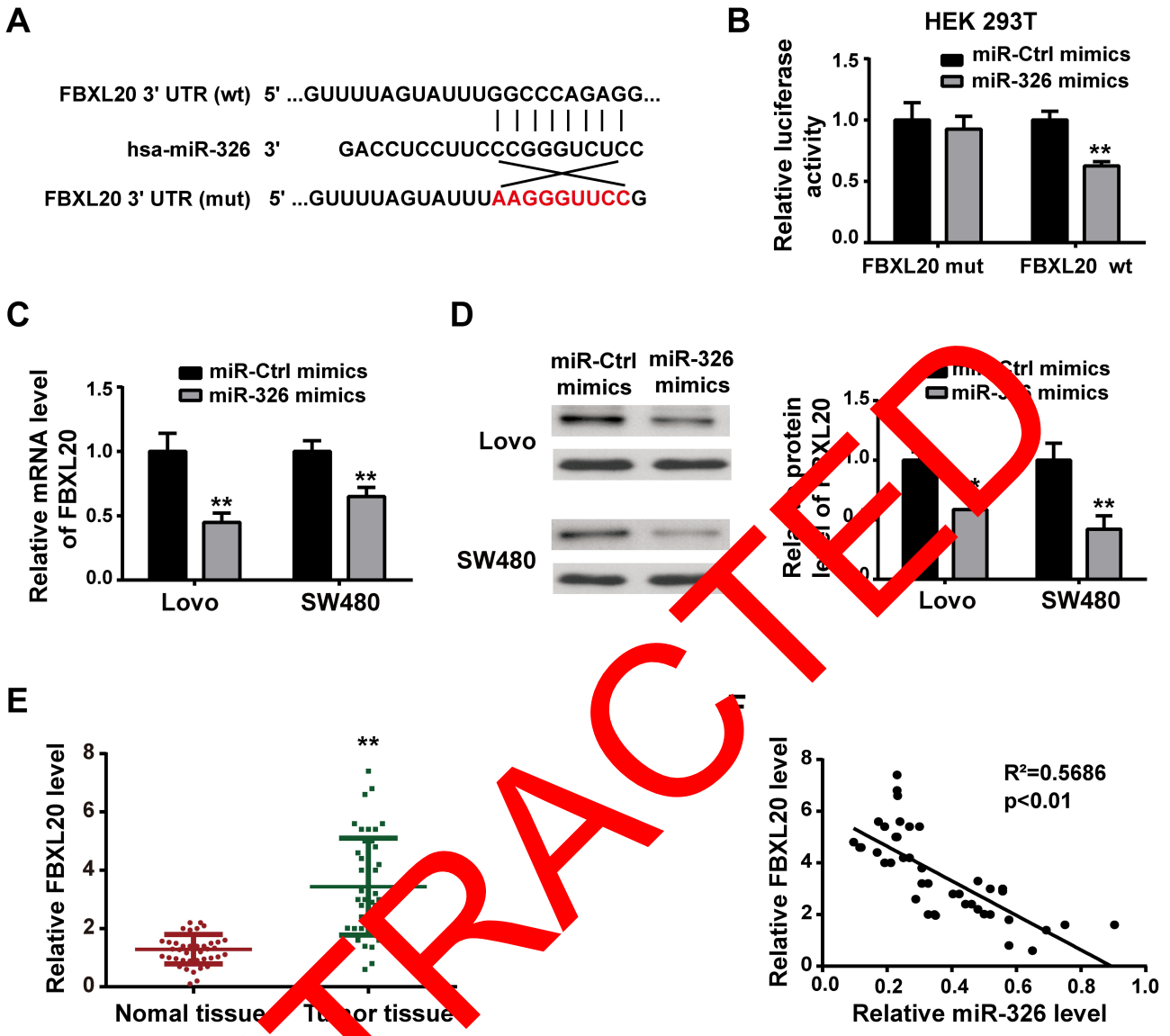

Figure 5 *miR-362* targeted *FBXL20* directly. (**A**) Binding sites between *miR-326* and *FBXL20* predicted by Target Scan were shown. (**B**) Luciferase report assay was performed in *HEK-293T* cells to verify the predicted binding sites. (**C**) Relative mRNA expression of *FBXL20* in CRC-3 and Du-145 cells were analyzed by qCRCR after *miR-326* mimics/miR-Ctrl mimics transfection. (**D**) Relative protein expression of *FBXL20* in CRC-3 and Du-145 cells were analyzed by qCRCR after *miR-326* mimics/miR-Ctrl mimics transfection. (**E**) Relative expression of *FBXL20* in CRC tissues and adjacent normal tissues were detected by qCRCR. (**F**) Negative correlation between *miR-326* and *FBXL20* in CRC tissues was analyzed by Pearson analysis. **P < 0.01 vs miR-Ctrl mimics or normal tissue.

Accumulating reports have demonstrated the lncRNA-miRNA-mRNA ceRNA network, in which lncRNAs compete for miRNAs thereby regulating target mRNA expressions.[21] A series of lncRNAs regulated colorectal cancer progression in this way, such as *TUG1*, *ZFAS1* and *LOC101927746*.[22–24] In order to investigate the mechanism of EWSA1-regulated CRC progression, we wanted to know whether lncRNA-miRNA-mRNA ceRNA network was involved. In the present study, we predicted *miR-326* as the target of *EWSAT1* with the help of bioinformatics methods. Previous reports showed that *miR-326* exhibited anticancer properties in various cancer types, such as osteosarcoma, hepatocellular carcinoma, cervical cancer and prostate cancer.[19,25–27] Moreover, increasing reports revealed that *miR-326* was regulated by lncRNA in multiple cancers. For example, lncRNA *KCNQ1OT1* promoted cell proliferation, differentiation and apoptosis by sponging *miR-326* to regulate *c-Myc* in acute myeloid leukemia.[28] EWSAT1 facilitated cervical cancer progression via targeting *miR-326* to regulate *MAPK1* expression.[27] In our study, we predicted *miR-326* as the target of *EWSAT1* using bioinformatics tools and verified this prediction by luciferase reporter assay as well as RNA RIP assay. Moreover, we found that *miR326* expression was

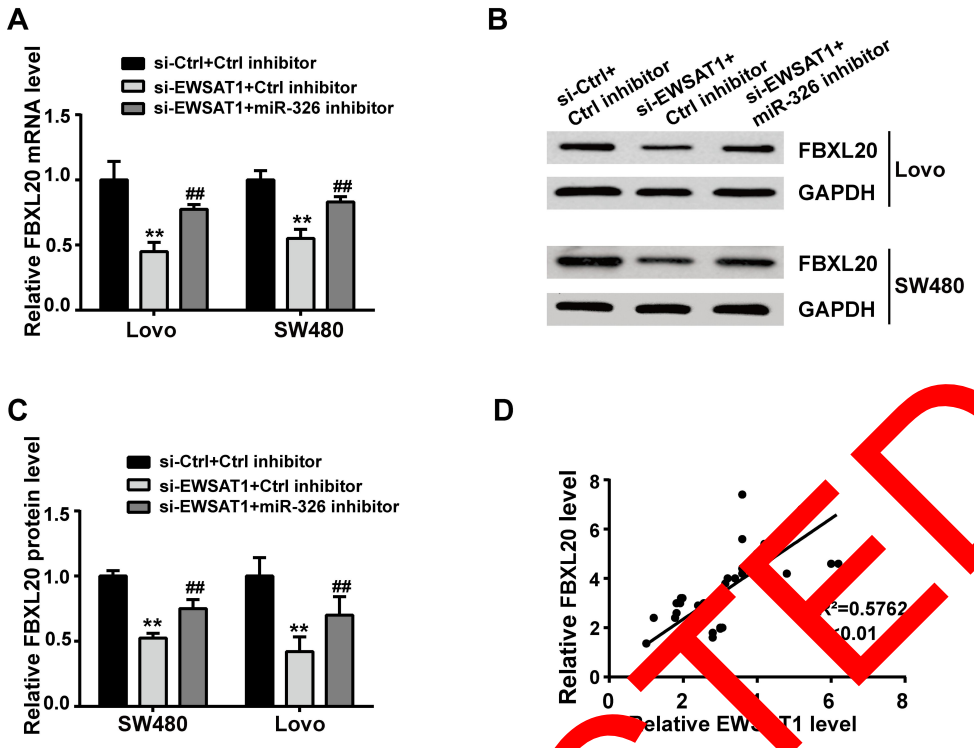

Figure 6 *FBXL20* was positively regulated by *EWSAT1* via *miR-326*. Si-EWSAT1 was co-transfected with either *miR-326* inhibitor or Ctrl inhibitor, (**A**) relative mRNA expression of *FBXL20* was estimated by qCRCR. (**B**–**C**) relative protein expression of *FBXL20* was analyzed by Western blot. (**D**) Positive correlation between *EWSAT1* and *FBXL20* in CRC tissues was analyzed by Pearson analysis. **P < 0.01 vs si-Ctrl+Ctrl inhibitor; ##P < 0.01 vs si-EWSAT1+Ctrl inhibitor.

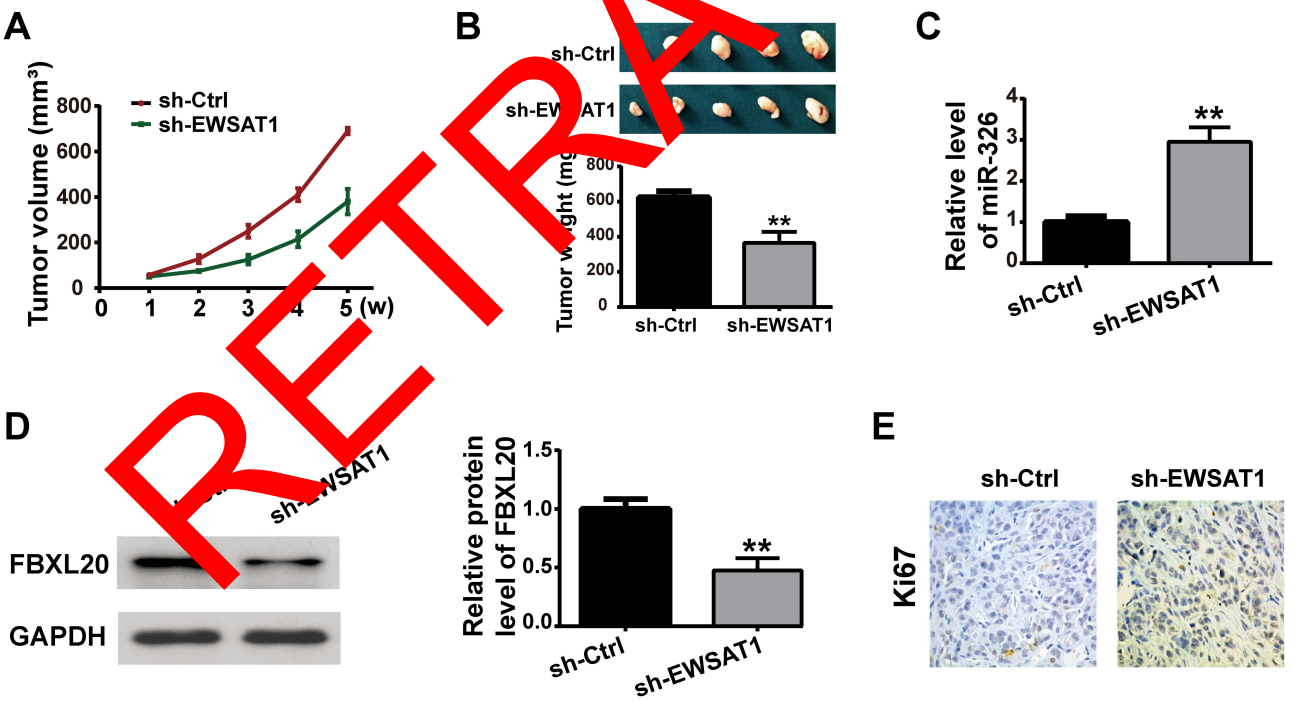

Figure 7 Knockdown of *EWSAT1* restricted tumorigenesis in xenograft models. Mice were inoculated with si-EWSAT1-transfected or si-Ctrl-transfected CRC-3 cells, (**A**) tumor growth curves were analyzed by measuring the tumor size weekly; (**B**) weight of tumor xenografts was measured five weeks later; (**C**) *miR-326* expression in tumor xenografts was analyzed by qCRCR; (**D**) *FBXL20* protein expression in tumor xenografts was determined by Western blot. (**E**) The proliferation marker *Ki67* in tumor xenografts was detected by IHC. **P < 0.01 vs sh-Ctrl.

negatively correlated with *EWSA1* in CRC tissues, and *miR-326* could reverse the inhibitory effects on CRC cell proliferation, migration and invasion induced by *EWSAT1* knockdown. Thus, our findings indicated that *EWSAT1* promoted CRC progression via sponging *miR-326*.

In addition, the most common mode of miRNAs functioning is to silence gene expression by binding to the 3′-UTR of targeted mRNAs. Thus, using bioinformatics tools, we predicted *FBXL20* as the target of *miR-326*. *FBXL20* was reported to be involved in some certain cancers. Eisfeld et al revealed that BAALC-driven acute myeloid leukemia via sponging *miR-3151* thereby upregulating *FBXL20*.[29] Zhu et al estimated *FBXL20* as an invasion inducer in colorectal adenocarcinoma.[30] Herein, we demonstrated that *FBXL20* was a direct target of *miR-326*, and negatively correlated with *miR-326* in CRC tissues. Moreover, *EWSAT1* positively regulated *FBXL20* via *miR-326* in CRC cell lines. All the data suggested that *EWSAT1* promoted CRC progression by targeting miR-326/FBXL20 axis. As we know that a lncRNA usually sponges different miRNAs, and a miRNA targets multiple protein-coding genes, more research is needed to study whether lncRNA *EWSAT1* can modulate other miRNAs and downstream target protein-coding genes. This will help us better understand the role of *EWSAT1* in colorectal cancer progression.

At present, the most commonly used tumor markers are tumor antigen and ectopic hormone. For example, carcinoembryonic antigen (CEA) was used for early diagnosis of colorectal cancer. However, there exist obvious shortcomings in traditional markers, including low specificity and sensitivity. The same marker can predict the possibility of multiple cancer risks, but also has a greater probability of missed diagnosis and misdiagnosis. LncRNAs have the following advantages compared with traditional biomarkers: Firstly, lncRNAs can exist stably in the circulatory system and has the characteristics of being free from nuclease degradation. Secondly, circulating lncRNAs can be detected in blood, urine and other body fluids by qPCR. Thus, we investigated the function of lncRNA in colorectal cancer progression. LncRNA *HOTAIR* is a well-known lncRNA associated with colon cancer. The high expression of lncRNA *HOTAIR* in blood is closely related to the mortality of colorectal cancer patients. ROC curve analysis showed that when the expression of lncRNA HOTAIR in serum was higher than 13.30, the sensitivity and specificity of diagnosing colon cancer were 65.96% and 85%, respectively. These results suggested that the expression of lncRNA *HOTAIR* in serum may be used in the diagnosis of colon cancer. As to lncRNA *EWSAT1*, we need further study to determine its clinical value.

In this study, we found that *EWSAT1* was upregulated in colorectal cancer tissues and cell lines. More importantly, through CCK8, colony formation, wound healing and transwell assays, we demonstrated that *EWSAT1* could promote colorectal cancer cell proliferation, migration and invasion by sponging *miR-326* and upregulating *FBXL20*.

Conclusions

All in all, we found that *EWSAT1* was highly expressed in CRC tissues and associated with poor clinical outcomes. Biological experiments revealed that knockdown of *EWSAT1* inhibited CRC cell proliferation, migration and invasion by modulating miR-326/FBXL20 axis, which might provide a novel therapeutic approach for CRC treatment.

Funding

This study was funded by Science and Technology Fund Project of Guizhou Health, Family Planning Commission (No. gzwjkj-2018-1-035), Science and Technology Fund Project of Guizhou Health and Family Planning Commission (No. gzwjkj-2018-1-075), Guizhou Science Project (Qian Science Foundation [2020] 1Y295) and National Natural Science Foundation of China (No. 82060523).

Disclosure

The authors report no conflicts of interest for this work.

References

1. Siegel RL, Miller KD, Goding Sauer A, et al. Colorectal cancer statistics, 2020. *CA Cancer J Clin*. 2020;70(3):145–164. doi:10.3322/caac.21601
2. Chen W, Zheng R, Baade PD, et al. Cancer statistics in China, 2015. *CA Cancer J Clin*. 2016;66(2):115–132. doi:10.3322/caac.21338
3. Veettil SK, Lim KG, Chaiyakunapruk N, et al. Colorectal cancer in Malaysia: its burden and implications for a multiethnic country. *Asian J Surg*. 2017;40(6):481–489. doi:10.1016/j.asjsur.2016.07.005
4. Rinn JL, Chang HY. Genome regulation by long noncoding RNAs. *Annu Rev Biochem*. 2012;81(1):145–166. doi:10.1146/annurev-biochem-051410-092902
5. Peng WX, Koirala P, Mo YY. LncRNA-mediated regulation of cell signaling in cancer. *Oncogene*. 2017;36(41):5661–5667. doi:10.1038/onc.2017.184
6. Marques Howarth M, Simpson D, Ngok SP, et al. Long noncoding RNA EWSAT1-mediated gene repression facilitates ewing sarcoma oncogenesis. *J Clin Invest*. 2014;124(12):5275–5290. doi:10.1172/JCI72124
7. Song P, Yin SC. Long non-coding RNA EWSAT1 promotes human nasopharyngeal carcinoma cell growth in vitro by targeting miR-326/-330-5p. *Aging (Albany NY)*. 2016;8(11):2948–2960. doi:10.18632/aging.101103

8. Zhou Q, Xie Y, Wang L, et al. LncRNA EWSAT1 upregulates CPEB4 via miR-330-5p to promote cervical cancer development. *Mol Cell Biochem*. 2020;471(1–2):177–188. doi:10.1007/s11010-020-03778-8
9. Sun L, Yang C, Xu J, et al. Long noncoding RNA EWSAT1 promotes osteosarcoma cell growth and metastasis through suppression of MEG3 expression. *DNA Cell Biol*. 2016;35(12):812–818. doi:10.1089/dna.2016.3467
10. Fu X, Zhang L, Dan L, et al. LncRNA EWSAT1 promotes ovarian cancer progression through targeting miR-330-5p expression. *Am J Transl Res*. 2017;9(9):4094–4103.
11. Renganathan A, Felley-Bosco E. Long noncoding RNAs in cancer and therapeutic potential. *Adv Exp Med Biol*. 2017;1008:199–222.
12. Chen S, Liu Y, Wang Y, et al. LncRNA CCAT1 promotes colorectal cancer tumorigenesis via A miR-181b-5p/TUSC3 axis. *Onco Targets Ther*. 2019;12:9215–9225. doi:10.2147/OTT.S216718
13. Gong A, Huang Z, Ge H, et al. The carcinogenic complex lncRNA DUXAP8/EZH2/LSD1 accelerates the proliferation, migration and invasion of colorectal cancer. *J BUON*. 2019;24(5):1830–1836.
14. Yu H, Ma J, Chen J, et al. LncRNA LINC00461 promotes colorectal cancer progression via miRNA-323b-3p/NFIB axis. *Onco Targets Ther*. 2019;12:11119–11129. doi:10.2147/OTT.S228798
15. Chen G, Gu Y, Han P, et al. Long noncoding RNA SBF2-AS1 promotes colorectal cancer proliferation and invasion by inhibiting miR-619-5p activity and facilitating HDAC3 expression. *J Cell Physiol*. 2019;234(10):18688–18696. doi:10.1002/jcp.28509
16. Ye T, Zhang N, Wu W, et al. SNHG14 promotes the tumorigenesis and metastasis of colorectal cancer through miR-32-5p/SKIL axis. *Vitro Cell Dev Biol Anim*. 2019;55(10):812–820. doi:10.1007/s11626-019-00398-5
17. Wilusz JE, Sunwoo H, Spector DL. Long noncoding RNAs: functional surprises from the RNA world. *Genes Dev*. 2009;23(13):1494–1504. doi:10.1101/gad.1800909
18. Caceres-Gutierez R, Herrera LA. Centromeric non-coding transcription: opening the black box of chromosomal instability? *Curr Genomics*. 2017;18(3):227–235. doi:10.2174/1389202917666161102095508
19. Moya L, Meijer J, Schubert S, et al. Assessment of miR-98-5p, miR-152-3p, miR-326 and miR-4289 expression as biomarker for cancer diagnosis. *Int J Mol Sci*. 2019;20(5):1154. doi:10.3390/ijms20051154
20. Zhang GY, Zhang JF, Hu XM, et al. Clinical significance of long non-coding RNA EWSAT1 as a novel prognostic biomarker in osteosarcoma. *Eur Rev Med Pharmacol Sci*. 2017;21(23):5337–5341.
21. Salmena L, Poliseno L, Tay Y, et al. A ceRNA hypothesis: the rosetta stone of a hidden RNA language? *Cell*. 2011;146(3):353–358. doi:10.1016/j.cell.2011.07.014
22. Yan Z, Bi M, Zhang Q, et al. LncRNA TUG1 promotes the progression of colorectal cancer via the miR-138-5p/ZEB2 axis. *Biosci Rep*. 2020;40(6). doi:10.1042/BSR20201025.
23. Chen X, Zeng K, Xu M, et al. SP1-induced lncRNA-ZFAS1 contributes to colorectal cancer progression via the miR-150-5p/VEGFA axis. *Cell Death Dis*. 2018;9(10):982. doi:10.1038/s41419-018-0962-6
24. Huang H, Cai L, Li R, et al. A novel lncRNA LOC101927746 accelerates progression of colorectal cancer by inhibiting miR-584-3p and activating SSRP1. *Biochem Biophys Res Commun*. 2019;509(3):734–738. doi:10.1016/j.bbrc.2018.12.174
25. Cao L, Wang J, Wang PQ. MiR-326 is a diagnostic biomarker and regulates cell survival and apoptosis by targeting Bcl-w in osteosarcoma. *Biomed Pharmacother*. 2016;84:825–835. doi:10.1016/j.biopha.2016.10.008
26. Wei LQ, Li L, Lu C, et al. Involvement of H19/miR-326 axis in hepatocellular carcinoma development through modulating TWIST1. *J Cell Physiol*. 2019;234(4):5152–5162. doi:10.1002/jcp.27319
27. Jiang H, Liang M, Wang Y, et al. The lncRNA TDRG1 promotes cell proliferation, migration and invasion by targeting miR-326 to regulate MMP13 expression in cervical cancer. *Cancer Cell Int*. 2019;19(1):152. doi:10.1186/s12935-019-0872-4
28. Cheng P, Lu P, Guan J, et al. LncRNA KCNQ1OT1 controls cell proliferation, differentiation and apoptosis by sponging miR-326 to regulate c-Myc expression in acute myeloid leukemia. *Neoplasma*. 2019;66(2):238–246.
29. Eisfeld AK, Marcucci G, Maharry K, et al. miR-3151 interplays with its host gene BAALC and independently affects outcome of patients with cytogenetically normal acute myeloid leukemia. *Blood*. 2012;120(2):249–258. doi:10.1182/blood-2012-02-408492
30. Zhu J, Deng S, Duan J, et al. FBXL20 acts as an invasion inducer and mediates E-cadherin in colorectal adenocarcinoma. *Oncol Lett*. 2014;7(6):2185–2191. doi:10.3892/ol.2014.2031